Resistance Noise in Electrically Biased Bilayer Graphene

Atindra Nath Pal* and Arindam Ghosh
Department of Physics, Indian Institute of Science, Bangalore 560 012, India
(Received 8 December 2008; published 25 March 2009)

We demonstrate that the low-frequency resistance fluctuations, or noise, in bilayer graphene are strongly connected to its band structure and display a minimum when the gap between the conduction and valence band is zero. Using double-gated bilayer graphene devices we have tuned the zero gap and charge neutrality points independently, which offers a versatile mechanism to investigate the low-energy band structure, charge localization, and screening properties of bilayer graphene.

DOI: 10.1103/PhysRevLett.102.126805 PACS numbers: 73.20.At, 74.40.+k, 81.05.Uw

The growing interest in bilayer graphene (BLG) is fueled by the ability to control the energy gap between its valence and conduction bands through external means [1–3]. The Bernal stacking of layers in BLG enforce strong interlayer coupling ($\gamma_1 \approx 0.35$ eV) at the adjacent atomic sites, leaving two low-lying states that form a zero gap semiconductor with quadratic dispersion. Setting finite potential difference between the layers opens a gap Δ_g between the bands, which can be tuned up to a maximum of $\approx \gamma_1$ using chemical doping [4,5], or application of an external electric field [6]. Consequently, biased BLG is not only attractive to nanoelectronics for device applications, but also forms a new and versatile platform for studying a wide range of phenomena including magnetic instabilities [7], or weak localization effects [8,9] with massive chiral Dirac fermions. However, intrinsic disorder has been suggested to modify the band structure in BLG as in conventional semiconductors by smearing the bands and localizing the states in band tails [10]. Most analyses assume disorder to be static, and the influence of any kinetics or time dependence of disorder on various properties of BLG is still poorly understood.

Recently, the low-frequency fluctuations, or the $1/f$ noise, in electrical resistance of bilayer graphene has been shown to be sensitive to its band structure [11]. The accepted mechanism of noise in graphene, as in carbon nanotubes [12], is connected to potential fluctuations from the trap states in the underlying silicon-oxide layers. In the case of monolayer graphene, the noise magnitude decreases with increasing carrier density (n) as the trap potentials are screened effectively by the mobile charges. Conversely, noise in BLG *increases* with increasing n, thereby forming a minimum around $n = 0$, which has been explained by the diminished ability of BLG to screen the external potential fluctuations in the presence of finite Δ_g. Indeed, theoretical models based on continuum self-consistent Hartree potential approach [2] or density-functional theory calculations [13] agree on maximal screening of the external potential as $\Delta_g \to 0$. Thus, low-frequency noise in BLG provides two crucial pieces of information: (1) interlayer charge distribution in the BLG since noise depends on the potential energy difference between the layers, and (2) the nature of single-particle density of states (DOS) as well as the chemical potential due to the sensitivity of noise to the underlying screening mechanisms. However, in noise experiments on BLG so far [11], Δ_g has been tuned only by varying n with a single (back) gate, where a partial screening of the gate potential leads to excess charge in the upper layer, and hence an electric field between the graphene layers [2]. Here, we have measured the low-frequency resistance noise in spatially extended double-gated BLG devices. The main objective is to achieve an independent tunability of Δ_g with both n and $\mathcal{E}$, where $\mathcal{E}$ is the transverse electric field across the electrodes, to separate the influence of band structure and carrier density on screening. Our experiments indicate that multiple processes involving the charge traps are active in producing the resistance noise which is intimately connected to the BLG band structure, being minimum at $\Delta_g = 0$ even if it corresponds to a nonzero n.

The bilayer graphene films were prepared on top of an n^{++}-doped Si substrate covered with $\approx$300 nm layer of SiO_2 by the usual mechanical exfoliation technique and identified with Raman spectroscopy. The double-gated devices [schematic in Fig. 1(a)] were prepared in the same way as outlined in Ref. [14]. Au leads were first defined by standard e-beam lithography technique. To form a top-gate dielectric layer, a thin layer of polymethyl methacrylate (PMMA, MW 950 K, 3% chlorobenzene) was spun onto the substrate, followed by cross-linking with exposure of 30 keV electrons at a dose of 21 000 μC/cm^2. Finally, a 40 nm thick Au gate was evaporated on top of the cross-linked PMMA covering the flake fully. The net carrier density on the BLG flakes is then given by $n = n_0 + \epsilon_{ox}V_{bg}/ed_{ox} + \epsilon_{cp}V_{tg}/ed_{cp}$, where n_0 is the intrinsic doping, ϵ_{ox} and d_{ox} are, respectively, the dielectric permittivity and thickness of the SiO_2 layer, while ϵ_{cp} and d_{cp} are those for the cross-linked polymer layer. The voltage applied on the back (doped silicon) and top (gold) gates are denoted as V_{bg} and V_{tg}, respectively. Typically, $d_{ox} \approx 300$ nm and $d_{cp} \approx 100$ nm

 © 2009 The American Physical Society

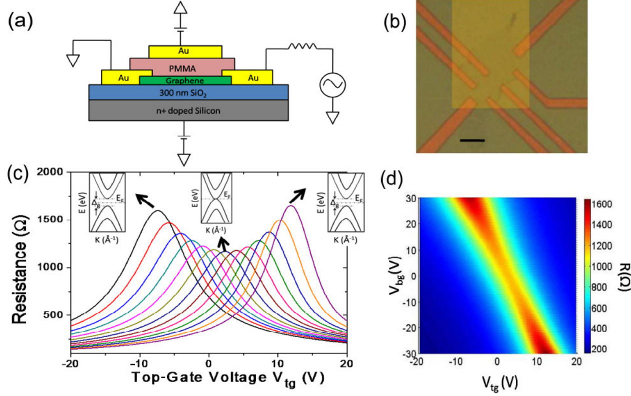

FIG. 1 (color online). (a) Schematic of the double-gated BLG device used in the experiment. (b) Optical micrograph of the device fabricated on the flake. The scale bar is 10 μm. (c) Resistance versus top-gate voltage for various backgate voltages, ranging from 30 to -30 V (left to right) with an interval of 5 V. Insets show schematics of corresponding band structures. (d) 2D color plot of the resistance as a function of both top gate and backgate voltages at $T = 107$ K, showing that the position of the charge neutrality peak shifts with both gate voltages according to the capacitance ratio.

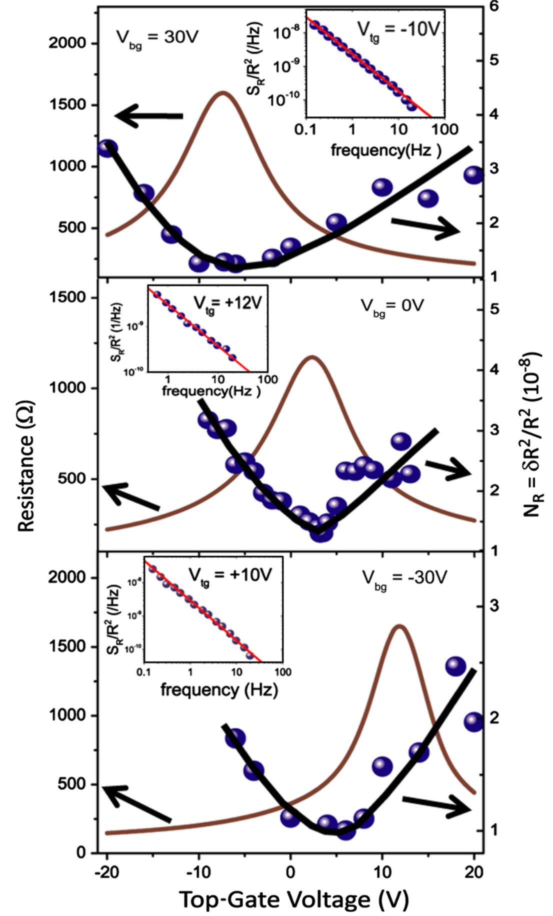

FIG. 2 (color online). Electrical transport and noise characterization of a BLG device. The resistance and the normalized noise power spectral density (N_R) as functions of top-gate voltages are shown for various backgate voltages: (a) 30 V, (b) 0 V, (c) -30 V. The thick solid lines are guides to the eye. The insets show typical noise power spectra S_R/R^2, far from the charge neutrality point for each backgate voltage.

were used which made the top gate about 3 times more effective in inducing carriers in the BLG devices than the backgate ($\epsilon_{ox} \approx 4$, $\epsilon_{cp} \approx 4.5$). For the device presented in this Letter, this was confirmed from the slope $dV_{tg}/dV_{bg} \approx 0.32$ [Fig. 1(d)] which tracks the shift in the resistance maximum occurring at the overall charge neutrality when both V_{tg} and V_{bg} are varied. The charge mobility of the device was estimated to be ~ 1160 cm^2/V s, which contained an intrinsic hole doping of $-n_0 \approx 5.82 \times 10^{11}$ cm^{-2}.

When V_{bg} and V_{tg} are different, a finite $\mathcal{E}$ is established between the electrodes. The maximum voltage difference was restricted to $|V_{bg} - V_{tg}|_{max} \lesssim 50$ V to avoid a dielectric breakdown. The resistance $(R) - V_{tg}$ characteristics of the device at $T \approx 107$ K are shown in Fig. 1(c) for several different values of V_{bg} spanning between -30 and $+30$ V. Existence of the electric field-induced band gap becomes increasingly prominent at higher V_{bg} with increasing R at charge neutrality (corresponding V_{tg} henceforth denoted as $V_{tg}^{R\max}$). Figure 1(c) also shows the $R - V_{tg}$ characteristics to be rather symmetric about $V_{tg}^{R\max}$ in our devices which indicates high degree of electron-hole symmetry, and confirms the material or quality of the contacts to be satisfactory for reliable noise measurements [15]. Noise in the BLG devices was measured in low-frequency ac technique with excitation below 500 nA (for details see Ref. [16]). For all noise measurements, the voltages to both gates were provided from stacks of batteries, which resulted in a background noise level within a factor of $\lesssim 2$ of the Nyquist level.

Typical power spectra of resistance noise are shown in the insets of Figs. 2(a)–2(c). For comparison, the resistance noise power spectral density, $S_R(f)$, is often normalized as $S_R(f) = \gamma_H(f)R^2/nA_Gf$, where γ_H is the Hooge parameter and $A_G \approx 72$ μm^2 is the area of the BLG flake between the voltage probes. We found $\gamma_H \sim 2 \times 10^{-3}$ sufficiently away from charge neutrality (at $n \sim 1.5 \times 10^{12}$ cm^{-2}), which is typical for semiconductor devices including BLG nanoribbons [11], and has been quantitatively modeled previously with either mobile defects [17] or time-dependent trapping phenomena [18–21]. Here, however, instead of focusing on γ_H or noise magnitude at a specific frequency, we compute and analyze the total variance of resistance fluctuations $N_R = \langle \delta R^2 \rangle / R^2 = (1/R^2) \times \int S_R(f)df$, which is essentially the normalized noise power spectral density integrated over the experimental bandwidth.

Figures 2(a)–2(c) show the variation of N_R and the corresponding average resistance as functions of V_{tg} at three different values of V_{bg}. For all V_{bg}, N_R shows a minimum at a specific V_{tg}, denoted as $V_{tg}^{N\min}$, and increases

monotonically on both sides of $V_{\rm tg}^{N\,\rm min}$. Similar behavior in BLG nanoribbons confirms this to be an intrinsic characteristic of BLG [11], although $V_{\rm tg}^{R\,\rm max}$ and $V_{\rm tg}^{N\,\rm min}$ are not equal in our measurements, indicating that noise minimum has been shifted away from charge neutrality in the presence of finite $\mathcal{E}$. In Fig. 3(a), we have plotted both $V_{\rm tg}^{N\,\rm min}$ obtained from noise measurements, as well as the corresponding $V_{\rm tg}^{R\,\rm max}$, at various $V_{\rm bg}$. As shown in Fig. 3(b), this allows us to follow the noise minimum point jointly with $n = n_\Delta = (\epsilon_0\epsilon_{\rm cp}/ed_{\rm cp})(V_{\rm tg}^{N\,\rm min} - V_{\rm tg}^{R\,\rm max})$, and external electric field $\mathcal{E} = \mathcal{E}_0 = (V_{\rm bg} - V_{\rm tg}^{N\,\rm min})/(d_{\rm ox} + d_{\rm cp})$.

Two features of Fig. 3(b) provide initial indication that minimum of N_R correspond to $\Delta_g = 0$. First, the analysis with self-consistent Hartree interaction of Ref. [2], which takes into account imperfect screening as well, shows that n_Δ and $\mathcal{E}_0$ are linearly related when $\Delta_g = 0$, as indeed observed experimentally. Secondly, the vertical dashed line at $\mathcal{E}_0 = 0$ identifies that a minimum in N_R occurs when the system is electron doped by the same amount as the intrinsic hole doping ($\approx n_0$), i.e., when the system is charge neutral, i.e., $\Delta_g = 0$.

To realize the implications of Fig. 3(b) quantitatively, we consider the case of unscreened BLG, where the gates induce equal charge densities at the BLG layers resulting in an interlayer electric field $= e(n_\Delta - n_0)/2\epsilon_0\epsilon_r$ at $n = n_\Delta$, where ϵ_r is the dielectric constant of the BLG region. The trap states in the substrate capture charge from BLG which have two effects: First, intrinsic doping of the BLG by $-n_0$ giving an additional interlayer field $= -en_0/2\epsilon_0\epsilon_r$, and secondly, the charged trap states would modify $\mathcal{E}_0$ by $\mathcal{E}_s = en_0/\epsilon_0\epsilon_{\rm ox}$. Hence, the variation of n_Δ with $\mathcal{E}_0$ in Fig. 3(b) can be deduced by setting the total electric field between the layers to be zero,

$$|\mathcal{E}_0 - \mathcal{E}_s| + \frac{e(n_\Delta - 2n_0)}{2\epsilon_0\epsilon_r} = 0. \quad (1)$$

Apart from confirming the band gap to be zero at the minimum of N_R, Fig. 3(b) and Eq. (1) provide several crucial insights. (1) *Charge organization:* Although we keep $V_{\rm bg}$ fixed and vary only $V_{\rm tg}$ to attain $n = n_\Delta$ in all

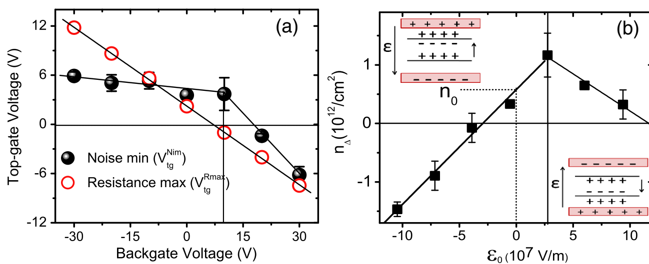

FIG. 3 (color online). (a) Top-gate voltages at charge neutrality point ($V_{tg}^{R\,\rm max}$) and noise minimum point ($V_{tg}^{N\,\rm min}$), plotted as functions of the backgate voltages, extracted from Figs. 1 and 2. (b) Dependence of charge density (n_Δ) on external electric field ($\mathcal{E}_0$) at the noise minimum point. n_Δ was calculated from the difference between the $V_{tg}^{R\,\rm max}$ and $V_{tg}^{N\,\rm min}$ (see text).

cases, the charge organization seems independent of this choice. Consequently, as shown in the insets of Fig. 3(b), directionally opposite effective electric fields can be screened at the same n_Δ by simply assuming the same doping with the opposite gate. This equivalence of the gates in spite of the difference in relative location with respect to the BLG is in keeping with the suggestion that, instead of a collection of two independent capacitor plates, the BLG must be viewed as a single active component [11], which in our case is electrostatically coupled to an assembly of two metallic electrodes. (2) *Screening:* In the presence of finite screening, Eq. (1) continues to be valid since screening modifies both external electric field and the excess charge density, leaving the linearity of n_Δ vs $\mathcal{E}_0$ at $\Delta_g = 0$ unaffected [2]. (3) *Dielectric constant:* The slopes of the lines on either side of $\mathcal{E}_0 = \mathcal{E}_s$ allow direct evaluation of the dielectric constant (ϵ_r) which we find to be $\epsilon_r \approx 1.7 \pm 0.2$ and $\approx 1.2 \pm 0.2$ for two opposite directions of effective external electric field [see insets of Fig. 3(b)]. While these values are reasonable [3], the difference may be due to the asymmetry in screening of disorder at the two configurations of charge distribution [insets of Fig. 3(b)].

The important remaining question concerns the microscopic mechanism of resistance noise in BLG, and, in particular, the role of charge traps in the substrate. In connection to this we have highlighted two aspects of BLG noise in Fig. 4. At first, the magnitude of $N_R^{\rm min}$ obtained at various $V_{\rm bg}$ was found to be surprisingly insensitive to corresponding n_Δ [Fig. 4(a)]. Since $\Delta_g = 0$ at the minimum of noise, this insensitivity suggests that the screening mechanism of external potential fluctuations remains largely unaffected as the charge density is varied at least over the range of $|n| \lesssim 10^{12}$ cm^{-2}, deviating significantly from simple calculations based on screened Coulomb potential in BLG and delocalized carriers [22]. To understand this we note that screening of an external potential is determined by the n dependence of local chemical potential, but in the proximity of charge traps, discrete charging or discharging of the trap states *locks* the chemical potential, making it insensitive to the gate voltage. Such a phenomenon has been observed in compressibility measurements in two dimensional systems close to the localization transition and attributed to dopant-related trap states [23]. Hence the weak variation in N_R also suggests that quasiparticles in our BLG device are possibly localized. Indeed, arbitrarily weak impurity potential has been suggested to smear the bands and localize the quasiparticles at low energies [24], particularly at the band tails, and experimental evidence of localized states in electrically biased BLG has been observed in low-temperature transport [6]. In our devices as well, we found the resistance at the charge neutrality point to increases with decreasing T irrespective of $\mathcal{E}$ (not shown), suggesting quasiparticles to be in the localized regime.

Among the models of low-frequency $1/f$ noise in systems with localized carriers, where charge transport takes

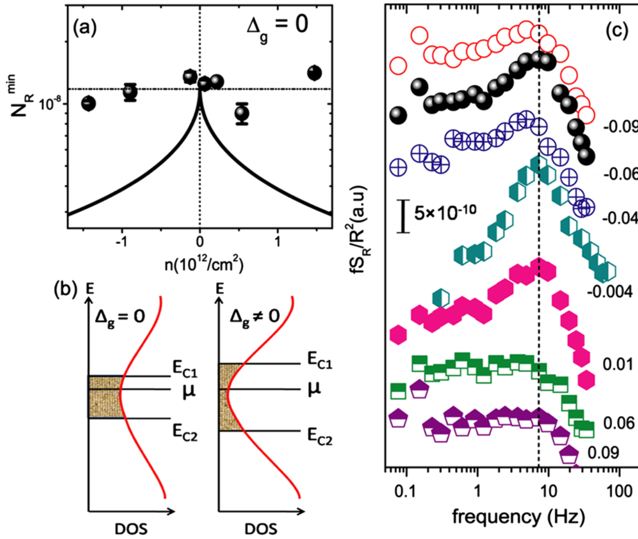

FIG. 4 (color online). (a) Variation of $N^R_{\rm min}$ with n. The solid curve shows the calculated noise as a function of n [see Ref. [17]). (b) Schematic representation shows the evolution of localization length ξ with increasing gap, where E_{C1} and E_{C2} are the mobility edges. (c) $fS_R(f)$ at the noise minimum ($\Delta_g = 0$) for various electric fields (V/nm), all of which show existence of a peak at $f \approx 7$ Hz. Individual traces have been shifted vertically for clarity.

place through nearest-neighbor (high T) or variable-range hopping (low T), both charge number fluctuations in the percolating cluster [18] or energy-level modulation in the hopping sites [19,20] have been discussed extensively. We believe both mechanisms are effective in our BLG devices. (1) The minimum of noise at $\Delta_g = 0$ may be understood from the sensitivity of noise to screening of the energy-level modulation of sites that do not belong to the percolation cluster. With increasing Δ_g, the localization length $\xi \sim \hbar/(2m^*|E_C - \mu|^{1/2})$ decreases [see schematic of Fig. 4(b)], since the mobility edge (E_C) increases with increasing band gap (and μ remaining nearly constant). This results in weaker screening, and hence higher resistance noise. (2) Secondly, the theoretical framework of noise from a slow charge-exchange process between the percolation cluster and the trap states predicts a saturation of the power spectral density at very low frequencies [18,21]. To verify this we have plotted $fS(f)$ as a function f in Fig. 4(c) at $\Delta_g = 0$ for various $\mathcal{E}_0$. Evidently, the low-frequency saturation in $S(f)$ manifests as peaks in $fS(f)$ indicating the crossover frequency $\sim\nu_0 \exp(-\sqrt{2/\pi n_0 \xi^2})$ to be $\approx$7 Hz, where $\nu_0 \sim 10^{13}$ Hz. This gives a reasonable estimate of $\xi \sim 0.5$–0.6 nm, within a factor of 2 of the effective Bohr radius of BLG. A coincidental clustering of trap capture rates around $\sim$7 Hz is unlikely due to the amorphous nature of the substrate oxide, although a systematic T dependence of noise is required to rule out this possibility. It is unclear though why the charge-exchange mechanism is best detectable for low $|\mathcal{E}_0|$, but its experimental signature, along with the locking of the chemical potential at low densities, provides a consistent framework to understand the role of disorder in the electronic and thermodynamic properties of BLG.

In conclusion, we have measured the low-frequency resistance noise in bilayer graphene flakes as a function of charge density and interelectrode electric field. The absolute magnitude of noise is intimately connected with the BLG band structure, and shows a minimum when the band gap of the system is zero. The experiments also reveal the charge organization in BLG-based electronic devices and the microscopic mechanism of resistance noise.

We acknowledge the Department of Science and Technology (DST) for a funded project, and the Institute Nanoscience Initiative, IISc, for infrastructural support. A. N. P. thanks CSIR for financial support.

*atin@physics.iisc.ernet.in

[1] E. McCann and V. I. Falko, Phys. Rev. Lett. **96**, 086805 (2006).
[2] E. McCann, Phys. Rev. B **74**, 161403(R) (2006).
[3] E. V. Castro *et al.*, arXiv:0807.3348v1.
[4] E. V. Castro *et al.*, Phys. Rev. Lett. **99**, 216802 (2007).
[5] T. Ohta *et al.*, Science **313**, 951 (2006).
[6] J. B. Oostinga *et al.*, Nature Mater. **7**, 151 (2008).
[7] T. Stauber, N. M. R. Peres, F. Guinea, and A. H. Castro Neto, Phys. Rev. B **75**, 115425 (2007).
[8] R. V. Gorbachev *et al.*, Phys. Rev. Lett. **98**, 176805 (2007).
[9] M. Koshino, Phys. Rev. B**78**, 155411 (2008).
[10] V. V. Mkhitaryan and M. E. Raikh, Phys. Rev. B **78**, 195409 (2008).
[11] Y. Lin and Phaedon Avouris, Nano Lett. **8**, 2119 (2008).
[12] Y. Lin, J. Appenzeller, J. Knoch, Z. Chen, and P. Avouris, Nano Lett. **6**, 930 (2006).
[13] H. Min, B. Sahu, S. K. Banerjee, and A. H. MacDonald, Phys. Rev. B **75**, 155115 (2007).
[14] D. Goldhaber-Gordon *et al.*, Phys. Rev. Lett. **98**, 236803 (2007).
[15] B. Huard, N. Stander, J. A. Sulpizio, and D. Goldhaber-Gordon, Phys. Rev. B **78**, 121402(R) (2008).
[16] A. Ghosh and A. K. Raychaudhuri, Phys. Rev. Lett. **84**, 4681 (2000); A. Ghosh *et al.*, arXiv:condmat/0402130.
[17] J. Pelz and J. Clarke, Phys. Rev. Lett. **55**, 738 (1985).
[18] B. I. Shklovskii, Solid State Commun. **33**, 273 (1980).
[19] V. I. Kozub, Solid State Commun. **97**, 843 (1996).
[20] V. Ya. Pokrovskii, A. K. Savchenko, W. R. Tribe, and E. H. Linfield, Phys. Rev. B **64**, 201318(R) (2001).
[21] B. I. Shklovskii, Phys. Rev. B **67**, 045201 (2003).
[22] E. H. Hwang and S. Das Sarma, Phys. Rev. Lett. **101**, 156802 (2008). Noise is estimated in *local interference* model with a screened Coulomb potential $\phi(r) \sim \sin(2k_F r)/(2k_F r + Cq_{\rm TF} r)^2$, at large distances r, where $q_{\rm TF}$ is Thomas-Fermi screening wave vector and C is a numerical constant.
[23] S. Ilani, A. Yacoby, D. Mahalu, and Hadas Shtrikman, Phys. Rev. Lett. **84**, 3133 (2000).
[24] J. Nilsson and A. H. Castro Neto, Phys. Rev. Lett. **98**, 126801 (2007).